

Abundance of Light Nuclei in the Primary Cosmic Radiation

M. V. K. APPA RAO, S. BISWAS, R. R. DANIEL, K. A. NEELAKANTAN, AND B. PETERS
Tata Institute of Fundamental Research, Bombay, India

(Received January 2, 1958)

The composition of the primary cosmic radiation is modified as a result of nuclear collisions which particles suffer in transit through the interstellar medium. The most sensitive indicator for the frequency of such collisions is the number of nuclear fragments corresponding to lithium, beryllium, and boron, which are found in the incident radiation close to the top of the atmosphere. It is, however, difficult to determine what fraction of these particles originated in outer space and what fraction is due to additional nuclear collisions in the uppermost layers of the atmosphere above the point of observation. In order to determine the relative importance of these two components, we have measured the percentage of light elements in the primary cosmic radiation as a function of the amount of air traversed by the particles. Our measurements are based on an analysis of 651 particle tracks recorded at geomagnetic latitude $\lambda=41^\circ$. The relative intensities obtained under air masses varying from 8.5 to 30 g/cm² are in good agreement with individual values for vertically incident particles obtained by other workers. Our data were obtained at a rather great altitude (6.6 g/cm² of residual pressure), so that they permit an extrapolation to the top of the atmosphere which is

largely independent of assumptions regarding the collision cross sections and fragmentation probabilities of complex nuclei. We have obtained the following primary flux values, in particles/m² sec sterad:

Li, Be, B (<i>L</i> nuclei)		0.55±0.60
C	2.65±0.40	
N	1.90±0.35	
O+F	3.00±0.45	
C, N, O, F (<i>M</i> nuclei)		7.55±0.65
$Z \geq 10$ (<i>H</i> nuclei)		2.20±0.35

Thus Li, Be, and B nuclei represent but a small fraction of the flux of heavy primary particles.

In order to account for this composition, the amount of interstellar gas traversed by the particles since their initial acceleration cannot have exceeded 1 g/cm² of hydrogen, as will be shown in detail in a separate paper. The smallness of this value imposes very stringent conditions on acceptable theories for the acceleration and subsequent diffusion of cosmic-ray particles.

I. INTRODUCTION

SOON after the discovery of complex nuclei in the primary cosmic radiation, it was suggested^{1,2} that the relative abundance of various elements among the primary nuclei could give information, not only on the chemical composition of the region where the particles originate, but also on their subsequent history. It was pointed out that in traversing interstellar space, the charge spectrum of the primary cosmic radiation must slowly shift toward lighter elements as a result of the partial destruction of heavy nuclei in collisions with nuclei in the interstellar gas. This process of fragmentation is known to happen in a fairly random manner, so that all nuclei lighter than the original one will occur as fragments. In particular, nuclear residues with charge number 3, 4, and 5 occur frequently in the collision between protons and complex nuclei and must, therefore, occur frequently in interstellar collisions of heavy primaries. A measurement of the abundance of the corresponding elements, namely, Li, Be, and B, among the primary particles, can then be used to put an upper limit on the percentage of heavy nuclei which have suffered collisions in interstellar space.

The natural abundance of Li, Be, and B (which we shall designate as *L* nuclei) is very low in those parts of the universe which are accessible to analysis. Suess and Urey³ estimate one such nucleus for 3×10^8 protons. It is, therefore, extremely likely that every *L* nucleus observed in cosmic rays represents the surviving frag-

ment of some heavier nucleus which suffered a collision in outer space, and that the intensity of *L* nuclei at the top of the atmosphere not only yields an upper limit to, but is in fact a fairly accurate measure of, the number of nuclear collisions suffered by the average cosmic-ray primary.

The number of collisions determines the amount of interstellar gas which the particles have traversed, starting with the time when their acceleration began and their energy had reached the few Mev/nucleon necessary for overcoming Coulomb repulsion, until the time at which they finally arrived at the outer boundary of our atmosphere. A knowledge of the amount of interstellar matter traversed by the primary radiation is of great importance for developing a consistent theory of the origin of cosmic radiation.

The earliest experiment² designed to determine the flux of Li, Be, and B nuclei in the primary cosmic radiation was carried out at geomagnetic latitude 30° , where nuclei arriving from the vertical direction have energies in excess of 3.5 Bev/nucleon. The ratio of Li, Be, B (*L* nuclei) to C, N, O, F (*M* nuclei) at the top of the atmosphere was found to be $R_0=L(0)/M(0) \leq 10\%$. The statistical accuracy of the measurement was not sufficient to set a lower limit. Since then 26 papers⁴⁻²⁹ have appeared dealing with similar measure-

⁴ Dainton, Fowler, and Kent, *Phil. Mag.* **42**, 317 (1951).

⁵ E. P. Ney and D. M. Thon, *Phys. Rev.* **81**, 1069 (1951).

⁶ J. A. Van Allen, *Phys. Rev.* **84**, 791 (1951).

⁷ Dainton, Fowler, and Kent, *Phil. Mag.* **43**, 729 (1952).

⁸ Kaplon, Peters, Reynolds, and Ritson, *Phys. Rev.* **85**, 295 (1952).

⁹ K. Gottstein, *Phil. Mag.* **45**, 347 (1954).

¹⁰ Kaplon, Noon, and Racette, *Phys. Rev.* **96**, 1408 (1954).

¹¹ T. H. Stix, *Phys. Rev.* **95**, 782 (1954).

¹ H. L. Bradt and B. Peters, *Phys. Rev.* **77**, 54 (1950).

² H. L. Bradt and B. Peters, *Phys. Rev.* **80**, 943 (1950).

³ H. E. Suess and H. C. Urey, *Revs. Modern Phys.* **28**, 53 (1956).

ments at various latitudes. Most of these refer to experiments using nuclear emulsions.

In the beginning there were many discrepancies between the results of different investigators, mostly due to specific experimental difficulties. In later work, these difficulties have largely been overcome and we shall show that practically all major investigations carried out at or close to latitude $\lambda \sim 41^\circ$ in recent years at various atmospheric depths, x , yield ratios $R(x) = L(x)/M(x)$ which are in very good agreement with each other. However, there is no agreement as yet on how to correct for atmospheric effects and, therefore, no agreement as to how much of the observed flux of light nuclei is incident from outside and how much must be attributed to the fragmentation of complex nuclei in the uppermost layers of the atmosphere.

Because of this difficulty, the ratios of L to M nuclei at the top of the atmosphere given in the literature range from zero to one, with most values clustering around 0.3 to 0.4. This spread of results obscures their astrophysical significance almost completely and justifies a new experiment in which all the customary techniques and the interpretation of measurements are subjected to re-examination.

II. EXPERIMENTAL PROCEDURES

Recently a number of excellent and very detailed papers have appeared which describe experiments to determine the composition of primary radiation with the aid of nuclear emulsions exposed in the stratosphere near geomagnetic latitude $\lambda = 41^\circ$. Particularly, in the papers of Waddington²⁶ and the Torino group of Cester *et al.*,²⁸ the important experimental problems which affect the detection and identification of heavy primaries and the resolution of the charge spectrum have been discussed with great care. Our experimental procedure was in many ways quite similar to that used by these authors, and although we have introduced a number of additional safeguards against experimental

¹² B. Waldskog, *Arkiv Fysik* **7**, 475 (1954).

¹³ Hourd, Fleming, and Lord, *Phys. Rev.* **95**, 647 (1954).

¹⁴ B. Peters, *Proc. Indian Acad. Sci.* **40**, 230 (1954).

¹⁵ L. S. Bohl, thesis, University of Minnesota, 1954 (unpublished).

¹⁶ J. Linsley, *Phys. Rev.* **93**, 899 (1954).

¹⁷ Biswas, Peters, and Rama, *Proc. Indian Acad. Sci.* **41**, 154 (1955).

¹⁸ W. R. Webber and F. B. McDonald, *Phys. Rev.* **100**, 1460 (1955).

¹⁹ H. Yagoda, *Phys. Rev.* **99**, 1644 (1955).

²⁰ H. Fay, *Z. Naturforsch.* **100**, 572 (1955).

²¹ J. Linsley, *Phys. Rev.* **101**, 826 (1956).

²² W. R. Webber, *Nuovo cimento* **4**, 1285 (1956).

²³ H. Yagoda, *Bull. Am. Phys. Soc. Ser. II*, **1**, 229 (1956).

²⁴ P. H. Fowler, *Proceedings of the Oxford Conference on Extensive Air Showers*, 1956 (unpublished), p. 55.

²⁵ Noon, Herz, and O'Brien, *Nuovo cimento* **5**, 854 (1957).

²⁶ C. J. Waddington, *Phil. Mag.* **2**, 1059 (1957).

²⁷ Koshiba, Schultz, and Schein, *Proceedings of the Varenna Conference*, 1957 (unpublished).

²⁸ Cester, Debenedetti, Garelli, Quassiat, Tallone, and Vigone, *Nuovo cimento* **7**, 371 (1958).

²⁹ V. Y. Rajopadhye and C. J. Waddington, *Phil. Mag.* **3**, 19 (1958).

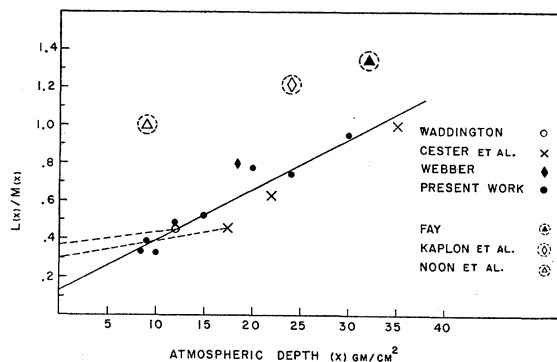


FIG. 1. The ratio of L nuclei (Li, Be, B) to M nuclei (C, N, O, F) as a function of atmospheric depth. The straight solid line is that of least-squares fit. The dashed lines indicate extrapolations used by Waddington²⁶ and Cester *et al.*,²⁸ respectively. Experimental points surrounded by circles are discussed in Appendix IV.

and observational errors, it seems sufficient to relegate the description of the methods to the Appendix. There we discuss in detail the procedures for determining scanning efficiency, calibration, and charge identification, as well as the various small corrections which must be applied to the charge spectrum as a result of the particular criteria used for accepting or rejecting various types of tracks. Except for minor details, our experiment differs from those of Waddington and the Torino group in two respects only:

1. It was carried out under a smaller weight of residual atmosphere, less than half as much as in their experiment. (The exposure lasted for $6\frac{1}{4}$ hours under 6.6 g/cm^2 of air plus 0.5 g/cm^2 of packing material.)

2. The number of tracks used for determining the charge spectrum (651 tracks of particles with atomic number $Z \geq 3$) is considerably larger than in all previous experiments. This makes it possible to obtain, separately, the composition for particles incident under various zenith angles. In this way we have determined the primary composition as a function of atmospheric thickness, x , in the interval $8.5 \leq x \leq 30 \text{ g/cm}^2$.

Leaving to the Appendix all details as to how the relative number of nuclei with different atomic number under various thickness of air was obtained, we proceed immediately to a discussion of the results and a comparison of our results with those of other workers.

III. EXPERIMENTAL RESULTS

In Fig. 1, we have plotted the experimentally determined ratio $R(x) = L(x)/M(x)$ of Li, Be, B nuclei (L group) to C, N, O, F nuclei (M group), as a function of atmospheric depth, x . We have included in the graph the results of all authors who measured this ratio at latitude $\lambda = 41^\circ$ or close to it (either by means of emulsions or by other techniques), and who have based their results on not fewer than 100 tracks of the medium (M) group. Figure 1 shows that the agreement between the different experiments is very good. A value reported

by Schein at the cosmic-ray conference in Varenna seems to be also in good agreement with the other measurements; it has been omitted only because the flight details have not yet been published. Five additional determinations of R have been published^{11,15,19,21,23} which have less statistical weight but are consistent with those plotted in Fig. 1. These have been omitted from the graph.

There are only three measurements (all of comparatively low statistical weight) which are in disagreement. The corresponding values have been included in the graph of Fig. 1, and have been surrounded by a circle. They are the experiments of Kaplon, Noon, and Racette,¹⁰ of Fay,²⁰ and of Noon, Herz, and O'Brien.²⁵ In each case it seems possible to give plausible reasons for the discrepancy which are discussed in Appendix IV.

We have chosen to compare here and in the other graphs ratios between different primary components rather than the absolute intensities for the following reasons:

1. Ratios (but not intensities) should be independent of slight differences in geomagnetic latitude and, therefore, also independent of differences in balloon trajectories.

2. Ratios (but not the absolute intensities) are independent of the shrinkage factor of emulsions, a quantity whose accurate determination is difficult and laborious.

3. Intensities under comparable thicknesses of air, but in different zenith directions, can be compared only if they are corrected for the variation of primary intensity with zenith angle at the top of the atmosphere.

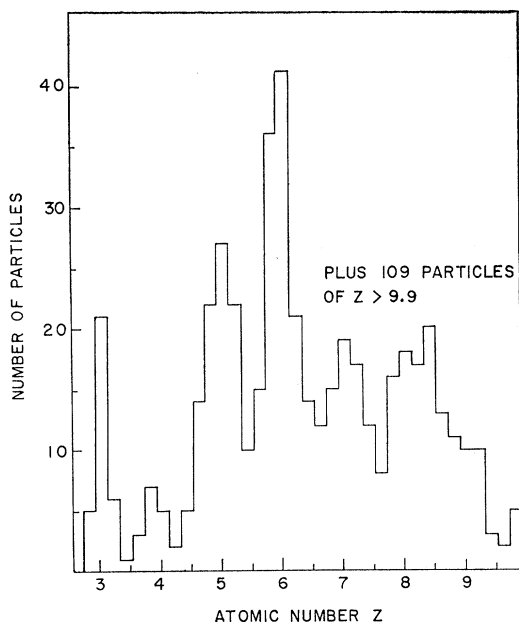


Fig. 2. Charge spectrum of particles with charge $Z \geq 3$ as deduced from grain density measurements in C-2 emulsions.

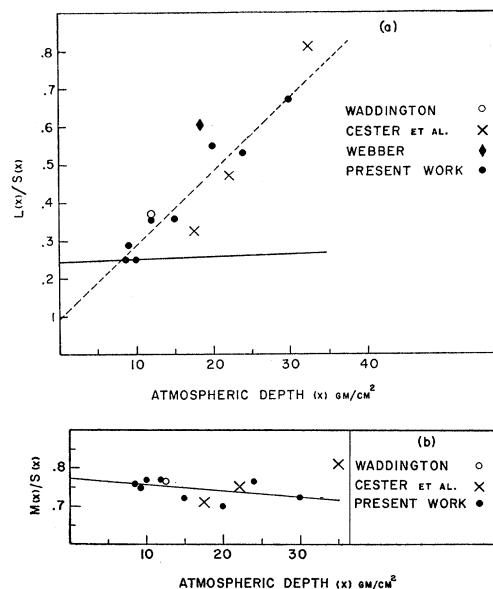


Fig. 3. (a) The ratio of L nuclei (Li, Be, B) to S nuclei ($Z \geq 6$) as a function of atmospheric depth. The dashed line is that of least-squares fit. The solid line indicates the expected change if the nuclei observed at 8.5 g/cm^2 consisted only of nuclei which have entered the atmosphere from the outside and no secondary particles are produced in the air. (b) The ratio of M nuclei (C, N, O, F) to S nuclei as a function of atmospheric depth.

Geomagnetic theory predicts a fairly large variation at latitude $\lambda = 41^\circ$, and the theory has not been checked with sufficient accuracy to make the corresponding corrections reliable. Intensity ratios between various components require no such correction.

The good agreement between the results of various experiments is not confined to the ratio $R(x) = L(x)/M(x)$. If one compares experiments with good statistics, one sees that it applies also the details of the primary charge spectra. Figure 2 shows our charge spectrum, which exhibits clearly a strong resemblance in its main features with the spectra published by Waddington²⁶ and the Torino group,²⁸ although the spectra were measured at different altitudes. In these three experiments carbon is the largest peak, followed by about equal numbers of nitrogen, oxygen, and boron. Next in intensity are small peaks of comparable size for fluorine, neon, lithium, and beryllium.³⁰

We therefore find reasonably consistent results, not only in the ratio $L(x)/M(x)$, but also when we form intensity ratios between various other primary components, for instance, the ratio of light (L), medium (M), or heavy (H) nuclei to the S group of primaries defined as comprising all nuclei with atomic number $Z > 5$. In Figs. 3(a) and (b), we show the ratios L/S and M/S as a function of atmospheric depth, x . In Fig. 4 (a), (b), and (c), we have plotted the ratios C/S , N/S ,

³⁰ Webber,²² however, who analyzes the primary spectrum with the help of a Čerenkov detector, obtains more Li and Be than B nuclei. He does not analyze the M and H groups.

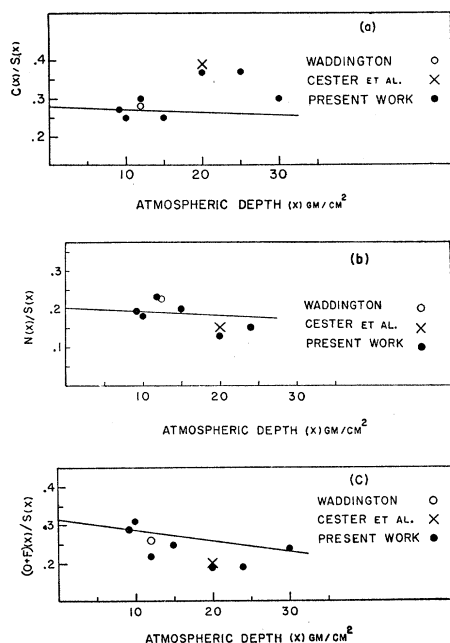


FIG. 4. Ratios of (a) carbon, (b) nitrogen, (c) oxygen and fluorine nuclei to S nuclei as a function of atmospheric depth. The solid lines indicate the expected change if the nuclei observed between 8.5 to 10 g/cm^2 were all primary particles.

and $(O+F)/S$. Again we have used all published data which are based on a minimum number of 100 M nuclei.

From these figures it appears that the observations on which the abundance of various components in the primary radiation must be based, are not in dispute.

IV. EXTRAPOLATION OF ABUNDANCE RATIOS TO THE TOP OF THE ATMOSPHERE

The dotted lines in Fig. 1 show the extrapolation used by some authors to obtain abundance ratios at zero atmospheric pressure. These extrapolations are based on a semitheoretical growth curve of light- compared to medium-weight primary components which evidently fits the experimental data rather poorly. There are several grounds on which this procedure of extrapolating the data can be criticized:

1. The growth curves which have been used involve a large number of parameters which have to be determined by experiment. These parameters are the mean free path for interaction of various primary nuclear components with atmospheric nitrogen and oxygen, and the probabilities of obtaining in such interactions surviving fragments of various sizes. Even if we classify all particles into only three groups [light (L), medium (M), and heavy (H)], there are still nine parameters which have to be measured: an interaction mean free path for each group, and fragmentation probabilities which determine whether a nucleus stays in its own group after collision or is transformed into a nucleus belonging to one of the light groups. Even if it were

possible to determine these nine parameters with fairly small individual errors, the combined effect of these errors on the calculated growth curve is so large as to destroy its usefulness.

2. The values which have been used for fragmentation probabilities have been determined on the basis of collisions observed in absorbers (mostly nuclear emulsions) whose atomic composition differs considerably from that of air.^{2,9,20,27-29,31,32} Attempts have been made to derive from these parameters, new parameters applicable to air, but they cannot be justified rigorously and lack a sound foundation in nuclear theory. In particular, it has often been assumed that a glancing collision of a primary with a heavy target nucleus in a nuclear emulsion leads to the same type of breakup as a head-on collision with a light target nucleus. It seems difficult to justify such an assumption.

3. Frequently, parameters measured at one latitude have been used to extrapolate data obtained at a different latitude. Yet it is possible that the fragmentation probabilities are energy-dependent.

For these reasons, it is not safe to rely on any of the proposed growth curves for the purpose of extrapolating data to the top of the atmosphere. It is necessary to measure the growth curve directly in air over the largest possible pressure interval and then use the experimental data for a semiempirical extrapolation to the top. The discrepancies between the primary flux ratios quoted by various authors are entirely due to differences in extrapolation procedures. The establishment of a reliable growth curve for the L component is, therefore, the crux of the problem.

In order to determine the flux of L nuclei at the top of the atmosphere, it is better to work with the ratio $L/S = L/(M+H)$ than with the ratios L/M or L/H , because L/S has a greater statistical weight and the procedure for extrapolation is easier to work out.

A. Straight-Line Extrapolation

In first approximation, one can simply draw a straight line representing a least-squares fit to the data of Fig. 3(a). Its intercept with the ordinate should be close to the true ratio at the top of the atmosphere, because as long as the atmospheric depth x at the points of observation is small compared to the interaction mean free path of the various nuclei whose collisions contribute to the L flux, the ratio L/S must increase linearly with x . The dashed line in Fig. 3(a) represents the least-squares fit to the data. Each point has been given a statistical weight proportional to the square root of the number of particles on which the corresponding measurement is based. The result, however, is almost independent of these weight factors.

The best-fitting straight line representing the data in Fig. 3(a) can be expressed by the equation:

$$r(x) = r_0 + \alpha x = 0.095 + 0.0193x. \quad (1)$$

³¹ J. H. Noon and M. F. Kaplon, Phys. Rev. **97**, 769 (1955).

³² Fowler, Hillier, and Waddington, Phil. Mag. **2**, 293 (1957).

This first approximation to an extrapolation yields, therefore, $L(0)/S(0) = 9.5\%$.

[If, instead of using only our data, we make use of all data at $\lambda = 41^\circ$ which have been published by various workers and which are based on at least 100 M nuclei, we obtain $(L_0/S_0) = 8.3\%$.]

In order to determine the probable error on this quantity, we divide the emulsion area and thereby our entire experiment into two equal parts containing 325 particles each and obtain a best-fitting line for each group separately. The lines intersect at $x_1 = 13.55 \text{ g/cm}^2$ and differ in slope by $\Delta\alpha = 0.0080$. The experimental uncertainty in the slope, α [Eq. (1)], should then be about half as large as the difference $\Delta\alpha$ between the slopes derived from the two partial experiments. We can, therefore, write for the straight-line approximation (including statistical error)³³

$$r(x) = r(x_1) + \alpha(x - x_1) = 0.356 + (0.0193 \pm 0.0040)(x - 13.55). \quad (2)$$

B. Accurate Extrapolation Formula

The intercept r_0 of the straight line drawn through the experimental points of Fig. 3 (a) gives, however, only an approximation to the flux ratios at the top of the atmosphere. The correct extrapolation formula is derived in Appendix V and yields:

$$R_0 = L(0)/S(0) = r_0 - \alpha(\delta_a + \delta_c). \quad (3)$$

Here δ_c is the term which arises from replacing the straight line by the real growth curve and δ_a is the term which arises from tracks recorded before the balloon reached ceiling.

δ_c is a simple function of \bar{x} and Λ , where \bar{x} is the point at which the straight line through the data is made tangent to the growth curve and Λ is the differential absorption mean free path of the L and S components defined by $1/\Lambda = (1/\Lambda_S) - (1/\Lambda_L)$. Since δ_c is always small, the precise value chosen for \bar{x} does not seriously influence the result.

δ_a is an important correction; it can be written in closed form and can be evaluated quite accurately because it depends only on the parameters of the flight (rate of ascent and length of stay at ceiling) and is insensitive to the choice of \bar{x} . Both functions are evaluated in Appendix V.

Not only the determination of *absolute* flux values but also the extrapolation of flux ratios to the top of the atmosphere requires, therefore, a knowledge of absorption mean free paths for heavy nuclei in air. Experimental data are available to determine these quantities with sufficient accuracy. They are discussed in the next section.

³³ This equation could of course also be written in the simpler form, $r(x) = r_0 + \alpha x$, but in this case, errors which are not independent of each other would have to be attached to both parameters, r_0 and α .

Our method of extrapolation does *not* require a knowledge of the so-called fragmentation probabilities (the probability that a collision between nuclei will lead to a fragment of a given size). This is an advantage because so far no experiments have been performed to determine these probabilities in materials similar in composition to that of air.

V. ABSORPTION MEAN FREE PATH OF HEAVY NUCLEI IN AIR

At latitude $\lambda = 41^\circ$, geomagnetic theory predicts a dependence of primary flux on zenith angle even when the flux is averaged over all azimuths. No extensive and accurate check of the theory has been made so far. For all latitudes higher than $\sim 20^\circ$ it seems, therefore, unsafe to deduce the absorption mean free path of primary nuclei from their variation of intensity with zenith angle. Near the equator, on the other hand, geomagnetic theory is probably reliable in its prediction^{34,35} that when the averaged over azimuth, the incoming radiation is isotropic for all zenith angles less than 70° . It seems, therefore, safe to derive the absorption mean free paths from the zenith angle dependence of flux observed at latitude $\lambda = 10^\circ$ by Danielson, Freier, Naugle, and Ney,³⁶ if we omit the last point of their data which represents measurements at zenith angle $\theta \gtrsim 70^\circ$.

A. Absorption of the M and S Components

Nuclei of particular elements will have a well-defined absorption mean free path provided their primary intensity is so high that contributions to their flux from the breakup of heavier elements can be neglected. Exponential absorption will also hold for strong *groups* consisting of elements of nearly equal atomic weights. For this reason, we may expect an exponential decrease in the atmosphere for the M component, comprising the elements C, N, O, and F. This is borne out by the measurements of Danielson and others³⁶ at 15 g/cm^2 pressure, and by the fact that their value $\Lambda_M = 26 \pm 2 \text{ g/cm}^2$ is in good agreement with similar measurements made at greater atmospheric depth. We shall, therefore, use the absorption mean free path Λ_M of these authors not only for $x > 15 \text{ g/cm}^2$ but also for the pressure interval $0 \leq x \leq 15 \text{ g/cm}^2$.

Since the M component is by far the strongest group among the nuclei heavier than boron, the S component which comprises both M and H nuclei will also to a good approximation be absorbed exponentially. We therefore use for Λ_S the value derived from the measurements of Danielson *et al.* at $\lambda = 10^\circ$ and zenith angles $\theta < 70^\circ$. This value is $\Lambda_S = 29.0 \pm 1.0 \text{ g/cm}^2$.

³⁴ The prediction is based on the curves given by Alpher³⁵ and on a primary energy spectrum of the form $N(>\epsilon) = K/\epsilon^{1.46}$, where ϵ represents particle energy including rest mass.

³⁵ R. A. Alpher, *J. Geophys. Research* **55**, 437 (1950).

³⁶ Danielson, Freier, Naugle, and Ney, *Phys. Rev.* **103**, 1075 (1956).

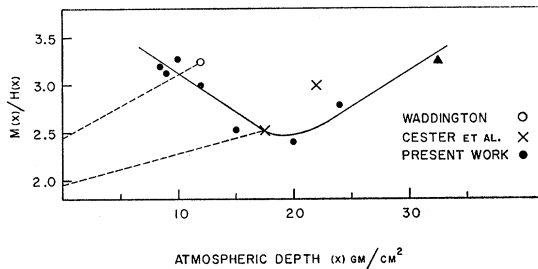


FIG. 5. The ratio of M nuclei (C, N, O, F) to H nuclei ($Z \geq 10$) as a function of atmospheric depth. The last point, marked \blacktriangle , was obtained by combining our own measurements with those of Cester *et al.*²⁸ The dashed lines indicate extrapolations used by Waddington²⁶ and Cester *et al.*²⁸

B. Absorption of the H Component

In contrast to the M and S components, the H component by itself does not follow an exponential absorption law. This arises from the fact that the group consists of nuclei of widely different weights ($20 \leq A \leq 60$). A large percentage of the *very* heavy nuclei in this group interact before they have penetrated 20 g/cm² of air; from emulsion work we know that in a high percentage of cases ($\geq 50\%$) such collisions leave large residues which must still be classified as H nuclei; in air the percentage must be larger. As a result, the absorption mean free path of the entire H component at very high altitude is at least twice as large as its interaction mean free path and is, therefore, *larger* than the absorption mean free path of the M component. This is borne out by our own observations and also by the measurements of Danielson *et al.*, who at 15 g/cm² obtained the absorption mean free path $\Lambda_H = 41 \pm 6$ g/cm². Ultimately, of course, after the traversal of more air, so that the internal composition within the H component has degenerated sufficiently, the absorption must become faster than that of the M component, and at greater atmospheric depth Λ_H must therefore become smaller than 26 g/cm². As a result of this particular and conventional way of subdividing complex primary nuclei, the ratio of M/H nuclei in the atmosphere first decreases and then, at an atmospheric depth greater than about 20 g/cm², it begins to increase. This trend is exhibited in Fig. 5.

C. Absorption Mean Free Path of the L Component

Unfortunately, no direct measurements exist on the absorption of L nuclei in air. We can make use of a semiempirical formula for the interaction cross section between two types of heavy nuclei, a formula which has been tested experimentally for incident nuclei ranging from helium to iron and for target materials of various atomic numbers ranging from glass to lead.^{1,2,8,28,29,31,32,37,38} This formula, originally given in

reference 1, can be written

$$\sigma_{1,2} = \pi r_0^2 (A_1^{\frac{1}{3}} + A_2^{\frac{1}{3}} - 1.17)^2 \text{ cm}^2, \quad (4)$$

where A_1, A_2 are the atomic weights of the colliding nuclei and r_0 has the value $r_0 = 1.45 \times 10^{-13}$ cm.

This cross section is defined as representing collisions in which the incident nucleus loses at least two units of charge. When applied to L nuclei in air, it therefore differs from the absorption cross section because it includes collisions in which a boron nucleus is transformed into a lithium nucleus; and at the same time it excludes collisions in which a lithium nucleus goes over into an α particle. Both types of collisions are comparatively rare and their effects will cancel to some extent. It therefore seems reasonable to use Eq. (4) for calculating the absorption mean free path Λ_L of the L component in air. The result is $\Lambda_L = 31.5$ g/cm².

Alternatively, we can try to determine Λ_L by using the nuclear radii measured by Hofstadter *et al.*,³⁹ and then estimate the percentage of collisions in which a L nucleus is transformed into a lighter nucleus still belonging to the L group. This probability is not well known; its value in nuclear emulsions is about 10%; and this leads to an absorption mean free path $\Lambda_L = 33.5$ g/cm², not very different from that obtained with the help of the semiempirical formula.

VI. FLUX RATIOS AND FLUX VALUES AT THE TOP OF THE ATMOSPHERE

A. Flux Ratios

We use the absorption mean free paths discussed in the previous section to calculate in Appendix V the correction term in Eq. (3), and obtain

$$\delta_e + \delta_a = \delta = 1.90 \pm 0.25 \text{ g/cm}^2; \quad \alpha\delta = 3.65\%.$$

The extrapolated flux ratio of L and S nuclei [Eqs. (2) and (3)] becomes

$$R_0 = 35.6 - (1.93 \pm 0.40)(\delta + 13.55)\% = 5.8 \pm 6.2\%. \quad (5)$$

As can be seen from the formulas, statistical fluctuations, which lead to a lowering of the extrapolated value for the uncorrected data, have the effect of increasing at the same time the ascent correction term. The effect of statistical fluctuations on the ascent corrected ratio is thereby magnified.

The ratio of Li, Be, and B to heavier primaries at the top of the atmosphere is quite small, most probably within the upper limit of 10% obtained in the earliest investigation. Within errors it could be slightly larger or it could be very much smaller. L nuclei registered during ascent play a substantial part in experiments using stratosphere balloons. This remains true regardless of the altitude at which the main exposure takes place.

The flux ratio M_0/S_0 at the top of the atmosphere

³⁷ Y. Eisenberg, Phys. Rev. **96**, 1378 (1954).

³⁸ F. B. McDonald, Phys. Rev. **104**, 1723 (1956).

³⁹ Hofstadter, Hahn, Knudsen, and McIntyre, Phys. Rev. **95**, 512 (1954).

can be derived in a manner entirely analogous to the one used so far. We get $M_0/S_0=0.775\pm 0.035$.

B. Absolute Flux Values

The *absolute* flux values can only be derived if we know the absorption properties of at least one of the components. Both the M and the S components decrease exponentially with increasing pressure. The absorption mean free paths are known with good accuracy (see Sec. V). The flux of M nuclei can be calculated either directly, or from the flux of S nuclei and the ratio M_0/S_0 ; the corresponding results are in good agreement. The flux of the H component is obtained from the flux of S nuclei and the ratio $H_0/S_0=1-(M_0/S_0)$. It can also be obtained from the flux of H nuclei at ~ 10 g/cm² and the knowledge that the absorption mean free path between 0 and 10 g/cm² must be close to but longer than the value obtained by Danielson *et al.* between 15 and 35 g/cm².

Individual flux values for the C, N, and O+F components are obtained by distributing the M flux among these nuclei in proportion to their frequency under 10 g/cm² of air, with a very minor correction to take into account the different sizes of the nuclei. The error introduced by the assumption that the composition *within* the M component does not change with atmospheric depth is probably small compared to the statistical errors.

Finally, we have calculated the extrapolated ratios L_0/M_0 and M_0/H_0 in order to facilitate comparison with other experiments. Our data are listed below:

Flux Values (particles/m ² sec sterad)	
L nuclei	0.55 ± 0.60
Carbon	2.65 ± 0.40
Nitrogen	1.90 ± 0.35
Oxygen plus fluorine	3.00 ± 0.45
M nuclei	7.55 ± 0.65
H nuclei	2.20 ± 0.35

Ratios
 $L_0/M_0 = (7.5\pm 8)\%$, $M_0/H_0 = 3.45\pm 0.65$.

VII. DISCUSSION OF RESULTS

The solid lines in Figs. 3 and 4 represent the expected change of primary composition with atmospheric depth on the assumption that the nuclei observed between 8.5 and 10 g/cm² of air are all truly primary particles.

Figure 4(c) shows that for oxygen plus fluorine this assumption must be close to the truth because the observed depth dependence agrees with the predicted one. (This is reasonable, because the oxygen peak itself is strong and there are no large peaks of heavier nuclei in the neighborhood which can contribute much to secondary oxygen production.)

The same holds true for nitrogen. The carbon ratio, C/S , increases perhaps a little faster with atmospheric depth than expected; thus there is an indication for a small contribution of secondary particles to the carbon

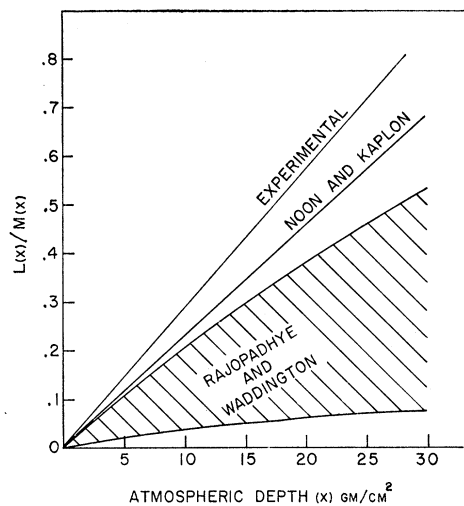


Fig. 6. The experimentally determined growth curve of the ratio L/M as a function of atmospheric depth, compared with growth curves calculated by Noon and Kaplon²¹ and Rajopadhye and Waddington.²⁹ The shaded region indicates the uncertainty in the theoretical curve as given by the last-mentioned authors.

peak which presumably comes from the neighboring strong group of N and O nuclei.

Figure 3(a) shows clearly that the growth curve of L nuclei is quite inconsistent with the assumption that the majority of nuclei observed between 8.5 and 10 g/cm² of air are truly primary particles.

In Fig. 6, the experimental growth curve of the L component is compared with the semitheoretical growth curves proposed by Noon and Kaplon²¹ and by Waddington,^{26,29} which are based on extrapolations from experiments carried out in nuclear emulsions. Waddington has also indicated the range of errors in the proposed curve. The measured growth curve is in closer agreement with that proposed by Noon and Kaplon²¹ than with that proposed by Waddington.

Table I, gives all published primary flux values at $\lambda=41^\circ$, extrapolated to zero pressure.

There is generally good agreement between various authors on the flux of S nuclei at geomagnetic latitude $\lambda=41^\circ$. This is to be expected because, as we have shown, the absorption of the S component in the atmosphere is truly exponential and therefore, apart from statistical errors, not very sensitive to the atmospheric depth from where the extrapolation to the top is carried out.

Our ratio M/H is significantly higher than that obtained by other authors and as a result, our value for the M flux is a little higher and for the H flux a little lower.

Since the high M/H ratio was measured at greater altitude than most other ratios listed in Table I, it should be more reliable. The discrepancy with previous measurements is presumably due to the fact that, as discussed in Sec. V, the absorption of the H component is not exponential but flattens out near the top, while

TABLE I. Extrapolated flux of M , H , and S nuclei at $\lambda \sim 41^\circ$.^a

Author(s)	Reference	Flux (particles/m ² sec sterad)			$\frac{M_0}{H_0}$
		M_0	H_0	S_0	
Van Allen (1951)	6	<6.0	<1.1	<7.1	...
Kaplon, Peters, Reynolds, and Ritson (1952)	8	5.9 \pm 0.7	2.4 \pm 0.3	8.3 \pm 0.8	2.46 \pm 0.43
Kaplon, Noon, and Racette (1954)	10	7.1 \pm 1.3	2.6 \pm 0.9	9.7 \pm 1.6	2.73 \pm 1.07
Stix (1954)	11	10.2 _{-3.4} ^{+4.5}	...
Yagoda (1955)	19	5.46 \pm 1.0	2.10 \pm 0.50	7.56 \pm 1.3	2.66 \pm 0.80
Linsley (1956)	21	7.4 \pm 1.7	4.2 \pm 2.0	11.6 \pm 2.6	...
Webber (1956)	22	9.20 \pm 1.20	...
Yagoda (1956)	23	4.37 \pm 0.63	2.22 \pm 0.45	6.59 \pm 0.80	1.96 \pm 0.50
Noon, Herz, and O'Brien (1957)	25	5.55	2.6	8.10	2.13
Waddington (1957)	26	6.10 \pm 0.60	2.50 \pm 0.30	8.60 \pm 0.67	2.44 \pm 0.38
Cester, Debenedetti, Garelli, Quassiat, and Tellone, and Vigone (1957)	28	5.52 \pm 0.40	2.82 \pm 0.40	8.34 \pm 0.57	1.96 \pm 0.31
Present work		7.54 \pm 0.65	2.22 \pm 0.35	9.86 \pm 0.75	3.45 \pm 0.65

^a The errors attached to our results are standard deviations. Most authors did not specify whether their errors refer also to standard deviation or to probable errors.

the M component is absorbed exponentially throughout the atmosphere. M/H decreases, therefore, at high altitude and increases at an atmospheric depth greater than ~ 20 g/cm². The curve in Fig. 5 illustrates this behavior of the ratio M/H in a qualitative way. The dotted lines, which represent the extrapolations made by Waddington²⁶ and by Cester *et al.*,²⁸ seem to lead to an underestimate of the flux ratios at the top of the atmosphere.

VIII. CONCLUSIONS

The various published measurements of the relative intensity of different primary components at latitudes close to $\lambda = 41^\circ$ and under air masses of various thicknesses are in good agreement with each other. This is true for all experiments of good statistics (more than 100 M nuclei), and for most of the measurements with lesser statistics. Three cases of comparatively low statistical weight give substantially different results but probable reasons can be given for the discrepancies.

The data establish a change of composition in the primary radiation with atmospheric depth which permits an extrapolation to the top of the atmosphere depending only on directly measurable quantities. Recent improvements in balloon performance made it possible to bring these measurements closer to the top of the atmosphere and thereby reduce the errors inherent in the corrections for secondary atmospheric effects. Separate flux values for C, N, and (O+F) nuclei have been obtained. Their combined intensities are in good agreement with the measurements of other authors. The intensity of nuclei with atomic number $Z \geq 10$, on the other hand, is somewhat lower than that estimated on the basis of measurements performed under greater thickness of air.

The primary flux of Li, Be, and B nuclei is $7.5 \pm 8.0\%$ of the flux of C, N, O, and F nuclei. Therefore, the conclusions about the origin of cosmic radiation which were drawn in an earlier paper² and which were based

on a ratio $L_0/M_0 \leq 10\%$ remain valid. Because of statistical errors it cannot be ruled out that the primary intensity of L nuclei is considerably smaller than the most probable value given above and it therefore seems that, as yet, the composition of the primary radiation cannot provide an argument against local, i.e., solar, theories for the origin of the radiation.

Statistics and resolution in this experiment were not sufficient to separate the fluorine from the oxygen flux. Since the natural abundance of fluorine must be expected to be extremely low,³ such a measurement could provide an independent check on the Li, Be, and B method for determining the amount of interstellar material traversed by primary cosmic-ray nuclei.

A thickness of the interstellar gas layer traversed by the average primary nucleus which is consistent with the observed intensity of the primary Li, Be, and B component will be calculated in a separate paper. It corresponds to less than 1 g/cm² of hydrogen.

ACKNOWLEDGMENTS

We thank the U. S. Office of Naval Research for having carried the emulsion stacks in their balloon flight, Mr. Yash Pal for having made the necessary arrangements for exposure, and Dr. M. G. K. Menon for useful discussions.

We also thank Mr. P. C. Mathur (now at the University of Delhi) and Mr. P. K. Sharma (now at the Panjab University) for help in the early part of this work, and Miss T. M. Purohit and Mrs. R. Rao for scanning some of the emulsions.

APPENDIX I. FLIGHT DATA, EMULSION STACKS, TRACK SELECTION CRITERIA, AND CORRECTION FOR SCANNING AND INTERACTION LOSSES

Flight Data

The balloon was launched at San Angelo, Texas (geomagnetic latitude $\lambda = 41^\circ$), on February 6, 1956.

Its rate of ascent was 3.32 meters per second. It reached a peak altitude of 34.7 km (6.2 g/cm^2), and floated for 6 hours and 15 minutes at a mean altitude of 34.2 km (6.6 g/cm^2). The flight curve is shown in Fig. 7.

Emulsion Stacks

The equipment consisted of three stacks of emulsion sheets, each of size $15 \times 20 \text{ cm}$ and 400μ thick. Two stacks were flown with emulsion surfaces vertical and each consisted of 8 C-2 emulsions flanked by two G-5 emulsions. The other stack was flown with emulsion surfaces horizontal and consisted of two G-5 emulsion sheets separated by 3 mm of celluloid. Only one vertical stack and the horizontal stack were used in this experiment.

The G-5 emulsions were developed for maximum sensitivity. Three of the C-2 emulsions in the vertical stack were processed to give normal sensitivity (25 times minimum ionization corresponded to nearly 70 grains/75 μ). The remaining C-2 emulsions were processed by using diluted amidol developer. They were not used in this experiment.

Selection Criteria

A. Vertical Stack

The G-5 emulsions on the outside of the stack were examined under a total magnification of $150\times$ for all tracks satisfying the following conditions:

1. All tracks must enter the stack from the upper hemisphere (any angle from $0^\circ \leq \theta \leq 90^\circ$).
2. The length of tracks projected into the plane of the emulsion must be greater than or equal to 1 mm per emulsion sheet.
3. Grain density must exceed that corresponding to

a particle with specific ionization six times larger than that of a singly charged particle at the minimum of ionization.

These tracks were traced through the stack until they led to an interaction or left the stack.

In order to be included in our analysis, a track must further satisfy the following criteria:

1. A track with a grain density greater than 60 grains/75 μ in C-2 emulsion must pass through at least the first three emulsions in the stack. This condition enables us to make δ -ray density measurements in at least one G-5 and grain density measurements in at least one C-2 emulsion.

2. Tracks with grain density less than 60 grains/75 μ in C-2 emulsion must satisfy the following conditions:

- (a) These tracks must have a minimum length of 1 cm in the stack.

- (b) Grain density must exceed that corresponding to a particle with a specific ionization eight times larger than that of a singly charged particle at minimum ionization (grain density > 30 grains/75 μ in C-2 and > 90 grains/75 μ in G-5 emulsions).

- (c) The grain density in the two G-5 emulsions must not differ by more than 6%. (At least 1000 grains were counted on each track. Reproducibility of counting results was better than 3%.)

These conditions eliminate all protons, deuterons, and tritons, but include α particles in the narrow energy range from 170 Mev to 270 Mev/nucleon which could be erroneously attributed to lithium nuclei. If such α particles exist, their effect would be to give a spuriously high value for the lithium flux. However, it is extremely unlikely that such α particles occur at $\lambda = 41^\circ$ in measurable numbers.

613 tracks in an area of 170.0 cm^2 satisfied all criteria.

B. Horizontal Stack

The upper G-5 emulsion was examined for tracks satisfying the following criteria:

1. The length of the track projected into the plane of emulsion sheet must be greater or equal to 1290 μ (this corresponds to a zenith angle $\geq 72\frac{1}{2}^\circ$).
2. The grain density must exceed that corresponding to a particle with a specific ionization six times larger than that of a singly charged particle at minimum of ionization.

Tracks satisfying the following conditions were selected:

1. Tracks with more than 2.5 δ rays/100 μ must traverse the top emulsion. (2.5 δ rays/100 μ corresponds to $Z = 5$.)

2. Tracks with less than 2.5 δ rays/100 μ must pass through both emulsions and their grain density must

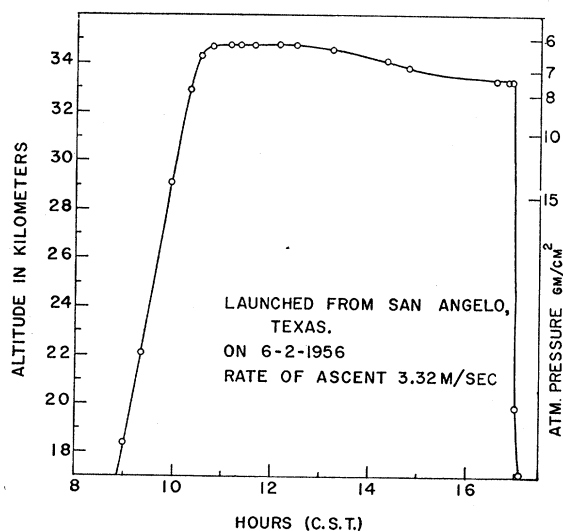


FIG. 7. Atmospheric pressure versus time for the balloon flight in which our emulsions were exposed. The rate of ascent was uniform at 3.32 m/sec.

TABLE II. Particle spectrum, with corrections.

Element	Li	Be	B	C	N	O	F	Z \geq 10	Total
Observed number	34	19	100	130	80	105	27	118	613
Scanning efficiency (%)	84.6	97.5	97.5	97.5	97.5	100	100	100	
Loss due to nuclear interactions (%)	6.4	7.0	4.4	4.7	5.1	5.3	5.6	6.5	
Corrected number of particles entering the stack	42.9	20.9	107.1	139.5	86.7	110.5	28.5	126.2	662.3

exceed 90 grains/75 μ . The difference in grain density in the two emulsions must not exceed 6%.

38 tracks in an area of 14.2 cm² satisfied all criteria.

Corrections

A. Correction for Particles Missed in Scanning Emulsions

It is a common difficulty in emulsion work that the lighter a nucleus, the harder it is to observe its track and to identify it as a primary against a background of slow secondary particles of comparable ionizing power and track density. Whatever the criteria for selecting tracks, the observations are always biased against finding and identifying light nuclei, in particular lithium.

In order to correct for this loss, the emulsion area scanned by each observer overlapped the area scanned by another observer. The overlap consisted of 50.9 cm² and contained 172 tracks (16 tracks of Li, 9 of Be, 22 of B, 93 of C, N, O, F, and 32 of nuclei with $Z \geq 10$). The number of tracks missed or misidentified by one but not by the other observer was 6 of Li and 4 of carbon. From this the efficiency correction for each observer was calculated in a straightforward manner. (The loss of the four carbon tracks has been distributed equally among Be, B, C, and N.) The average efficiencies are shown in Table II.

14.2 cm² in the horizontal stack were scanned by two observers whose efficiency for all types of nuclei in the vertical stack was 100%; therefore, no corrections were made.

B. Correction for Loss by Nuclear Collision

A particle may collide in the emulsion stack before its track satisfies the criteria regarding minimum track length. Corrections have been made for each charge separately using collision mean free paths in emulsion, calculated according to the relation given by Eq. (4) (Sec. V). The correction factors are given in Table II.

APPENDIX II. CHARGE DETERMINATION FROM δ -RAY AND GRAIN DENSITY MEASUREMENTS

Although grain density measurements can have higher statistical weight than δ -ray measurements, there is always a danger that nonuniformity in the sensitivity of nuclear emulsion introduces errors in the

ionization measurement and a corresponding distortion in the charge spectrum. δ -ray density measurements, on the other hand, do not depend strongly on the sensitivity of emulsions. Only if it can be shown that the uniformity of the emulsion used is adequate for the purpose, can one expect to obtain a satisfactory charge spectrum in C-2 emulsion for charges less than 9. For this reason we have made independent measurements both of grain density and δ -ray density on about half the tracks.

1. Charge Determination from δ -Ray Density Measurements

δ -ray density was measured in the G-5 emulsions of the vertical stack on 323 tracks of heavy primaries obtained in the first half of the total area scanned. The δ rays of each track were counted in the first as well as the last emulsion unless the particle interacted in between. All δ rays with four or more grains were counted. The consistency of δ -ray counts was checked by repeating measurements on tracks at random throughout the duration of the experiment; the results were consistent within 7.5%.

A plot of δ -ray density, $N_\delta/100 \mu$, versus number of tracks for these 323 tracks is shown in the histogram in Fig. 8. It exhibits a number of fairly well-resolved peaks. Before proceeding to identify the peaks we discuss the limit of resolution obtainable at latitude $\lambda = 41^\circ$.

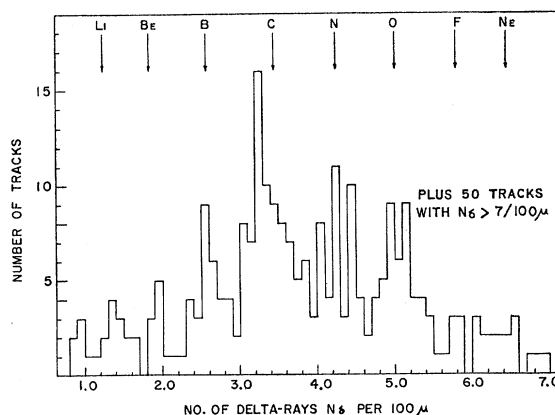


Fig. 8. δ -ray density distribution obtained from measurements made on 325 tracks of particles with charge $Z \geq 3$.

Resolution

The theoretically possible resolution for peaks in the δ -ray density distribution is obtained from the following considerations. The δ -ray density of particles incident at $\lambda=41^\circ$ from the vertical direction varies by 15.5% depending on particle energy. If, as in our experiment, all angles are included, the spread is somewhat larger (20%), because of lower energy particles coming from the west. The expected δ -ray distribution is shown in Fig. 9(a).^{40,41} It is based on a primary energy spectrum of the form $N(\geq \epsilon) = K/\epsilon^{1.45}$, ϵ representing particle energy including rest mass, and on the transcribed Mott formula⁴⁰ giving the number of δ rays as a function of particle velocity. The theoretical distribution is shown in Fig. 9(a), which agrees well with the experimental distribution for the strongest group. At $\lambda=41^\circ$, the

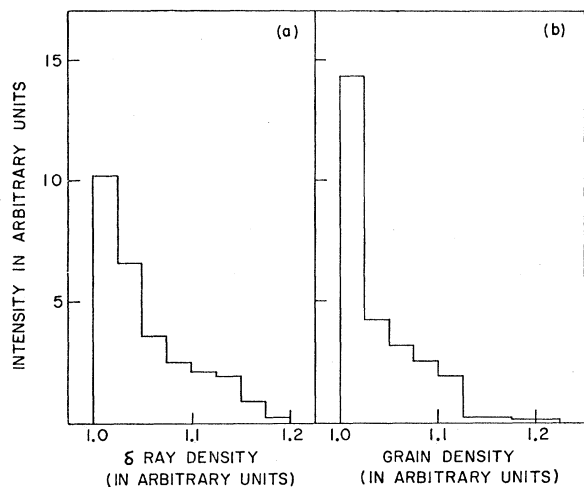


FIG. 9. The expected spread in the δ -ray density and grain density distributions for tracks of primary particles of a given charge arriving at $\lambda=41^\circ$ with an energy spectrum of the form $N(>\epsilon) = K/\epsilon^{1.45}$. Histogram (a) was calculated by using the (transcribed) Mott formula⁴⁰ for the variation of δ -ray density with energy. Histogram (b) was calculated by using the measurements of grain density versus energy given by Stiller and Shapiro.⁴¹

spread in the δ -ray distribution is therefore small enough so that it is just possible to resolve groups due to neighboring charges for all values up to $Z=14$.

For calibration purposes it is necessary to determine the most probable δ -ray density for particles of a given charge rather than rely on a single particle of unknown energy. It can be seen from Fig. 9(a) that the most probable δ -ray density is that corresponding to completely relativistic particles.

Charge Calibration

First we determined the relation between δ -ray density and charge for highly relativistic particles. For this purpose we used a stack (*N* stack) consisting of

⁴⁰ H. L. Bradt and B. Peters, Phys. Rev. 74, 1828 (1948).

⁴¹ B. Stiller and M. M. Shapiro, Phys. Rev. 92, 735 (1953).

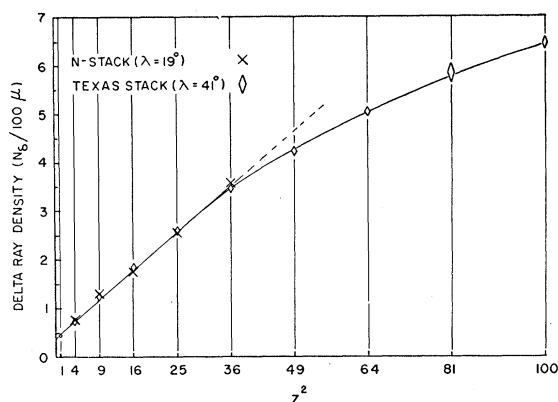


FIG. 10. δ -ray density versus square of the atomic number for very long tracks with energy >5 Bev/nucleon compared with that of particle tracks recorded at $\lambda=41^\circ$. The dotted line represents the relation $N_\delta = 0.088Z^2 + 0.35$. The vertical heights of the diamond symbols represent the standard deviations of the measurements.

200 G-5 emulsion sheets of thickness 600μ , which was flown at $\lambda=19^\circ$ where the cutoff energy is 5 Bev/nucleon. The emulsions were scanned for relativistic particles of charge $Z \geq 2$ with a minimum length of 1 cm per emulsion. 300-600 δ -rays were counted on each track. We found one event in which a very long track of a multiply charged particle splits into 3 α particles without giving rise to other charged particle tracks. This track must be identified as due to a relativistic carbon nucleus. Its δ -ray density was 3.50 ± 0.25 . Between the δ -ray density peaks corresponding to charge $Z=2$ and $Z=6$, we found three additional distinct groups of δ -ray density. These are, therefore, identified as due to particles with atomic numbers $Z=3, 4, \text{ and } 5$.

In the stack exposed at Texas we used long tracks (>2 mm per plate) whose δ -ray density corresponded to the distinct peaks in the distribution Fig. 8. The agreement between the δ -ray density peaks in both stacks is very close as shown in Fig. 10.

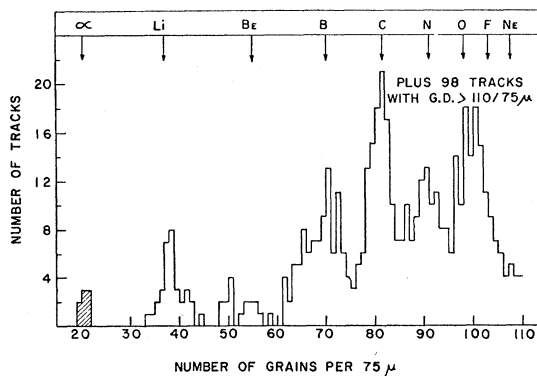


FIG. 11. Grain density distribution in C-2 emulsions of 595 tracks due to particles of charge $Z \geq 3$. For the sake of comparison we have also shown the grain density of eight relativistic α particles ejected from heavy primary collisions in emulsion (shaded area).

TABLE III. Comparison of charge determination from δ -ray density and grain density measurements. Total No. of tracks: 278.

1.	Charge group	Li	Be	B	C	N	O	F	$Z \geq 10$
2.	Number of tracks of particles identified by grain density measurements	14	8	40	72	40	41	14	49
3.	Number of tracks of particles identified by δ -ray density measurements	11	13	31	69	45	40	12	57
4.	Mean charge from δ -ray measurements for tracks identified by grain density measurements	3.01	4.30	5.33	6.17	7.01	8.37	8.5	...
5.	Mean charge from grain density measurements for tracks identified by δ -ray measurements	3.02	4.05	5.14	5.86	6.8	7.98	8.39	...

2. Charge Determination from Grain Density Measurements

It was found that the sensitivity of all C-2 emulsions in which measurements were performed was the same within experimental error ($\sim 3\%$). About 500 grains were counted on each track with grain density below 60 grains/75 μ and about 1000 grains on heavier tracks. The sections of track chosen for grain density determination were always distributed uniformly along its entire length in an emulsion. A plot showing number of tracks *versus* grain density of tracks is shown in Fig. 11. For comparison with the peak identified as lithium, we have also included in this figure grain counts on α particles emitted from breakup of heavy particles. Up to a grain density of 100 grains/75 μ the peaks are well resolved; beyond this, saturation sets in.

Resolution of Grain Density Peaks

The theoretically expected resolution of grain density peaks was calculated in the same manner as that of δ -ray density peaks, assuming an energy spectrum of $N(\geq \epsilon) = K/\epsilon^{1.45}$ and the experimentally determined curve of grain density *versus* energy given by Stiller and Shapiro.⁴¹ The theoretically expected histogram is shown in Fig. 9(b). It has nearly the same width as the main peak in the experimentally determined grain density distribution, Fig. 11.

Charge Calibration Based on Grain Density of Tracks

The C-2 emulsion was scanned for large stars in which some prongs could be followed into neighboring emulsions. Since the stack remained assembled only for about three weeks, there could not be any appreciable relative fading between the tracks associated with these stars and those of heavy primaries. Five tracks which were associated with these stars and which came to rest in the same emulsion sheet in which they originated and had residual ranges > 1.5 mm were selected for measurement. These were identified as protons by the method of constant-sagitta scattering.⁴² The grain density measurements on these tracks as a

⁴² Biswas, George, and Peters, Proc. Indian Acad. Sci. 38, 418 (1953).

function of residual range are shown in Fig. 12.⁴³ In the same figure we show the restricted energy loss as given by Barkas and Young⁴³ and the grain density of the first three prominent peaks in Fig. 11. It is seen that according to the restricted energy loss, the grain density peaks of Fig. 11 at 37, 70, and 82 agree excellently with those of Li, B, and C nuclei, respectively.

The grain density corresponding to the Li and the C peak shown in Fig. 11 are used to determine parameters, a and b , in an empirical relation giving the grain density: $g = aZ^2/(1+bZ^2)$. From this formula we infer that the grain density of B, N, and O should lie at 70, 91, and 98, respectively. This is in good agreement with the observed peaks. Individual charge values, not necessarily integral, were assigned with the help of this formula. The charge distribution is shown in Fig. 2.

3. Comparison of Charge Determinations from δ -Ray Density and Grain Density Measurements

A comparison of charge determinations from δ -ray density and grain density measurements was made for 278 tracks. Table III shows the mean charge, as determined from grain density in C-2 emulsions, of all

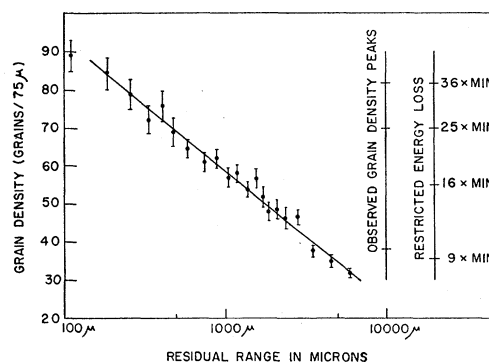


Fig. 12. Grain density in C-2 emulsions of proton tracks as a function of residual range. On the right we show the position of the first three well-resolved grain density peaks of Fig. 11, as well as the grain densities corresponding to a restricted energy loss of 9, 16, 25, 36 times minimum as given by Barkas and Young.⁴³

⁴³ W. H. Barkas and D. M. Young, University of California Radiation Laboratory Report UCRL-2579, 1954 (unpublished).

particles whose atomic number was determined on the basis of δ -ray densities of their tracks in *G-5* emulsions. It also shows the mean charge, as determined by δ -ray density, which had been identified on the basis of grain counts. It can be seen that the two methods of charge calibration used here are consistent and in good agreement up to $Z=8$. Statistically the δ -ray method is inferior to grain counting for particles $Z < 6$. Therefore, the charge values finally assigned to 595 of the tracks used in the experiment are those based on grain density measurements. For the remaining 38 tracks observed in the horizontal stack and 18 on which grain counting could not be made (owing to bad regions of the emulsion) in the vertical stack, the charges were estimated from δ -ray density measurements.

APPENDIX III. RATIO BETWEEN GROUPS OF NUCLEI AT DIFFERENT ATMOSPHERIC DEPTHS

We calculated for each particle, the total amount of matter traversed in the atmosphere (from the zenith angle) and the packing material (Bakelite of thickness 0.5 g/cm²). Tracks were then classified according to the amount of material traversed.

In order to minimize fluctuations due to the choice of arbitrary intervals when determining a ratio like $R(x) = L(x)/M(x)$, the following procedure was adopted. For each atmospheric depth y_0 , we computed from the number of tracks traversing various amounts of matter the quantity

$$r(y, y_0) = \int_{y_0}^y L(x) dx / \int_{y_0}^y M(x) dx \quad (6)$$

for different values of y . Then $r(y, y_0)$ is plotted against

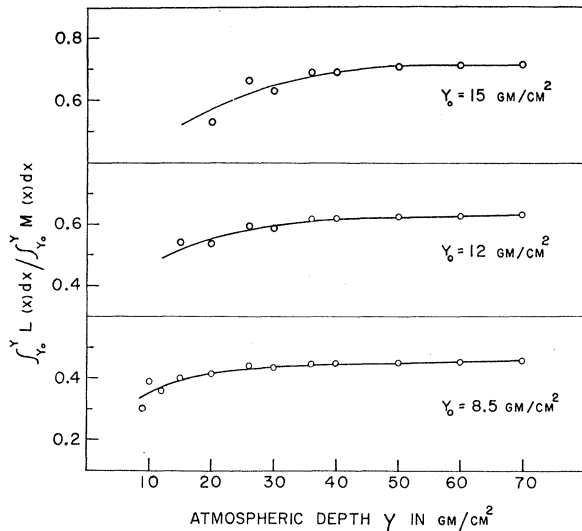


FIG. 13. Three typical curves for the quantity

$$r(y, y_0) = \int_{y_0}^y L(x) dx / \int_{y_0}^y M(x) dx$$

plotted against y for $y_0 = 8.5, 12, \text{ and } 15 \text{ g/cm}^2$.

y . As $y \rightarrow y_0$, $r(y, y_0)$ approaches $R(y_0) = L(y_0)/M(y_0)$. Three typical curves for $y_0 = 8.5, 12, \text{ and } 15 \text{ g/cm}^2$ are shown in Fig. 13. This procedure was then followed for determining other ratios such as $L/S, C/S, N/S, \text{ and } (O+F)/S$, (see Figs. 3 and 4).

APPENDIX IV. DISCUSSION OF MEASUREMENTS MADE BY KAPLON ET AL., NOON ET AL., AND FAY

Only three of the twelve L/M ratios obtained by various authors at or near $\lambda = 41^\circ$ are hard to reconcile with the line drawn in Fig. 1. All three are based on a fairly small number of particle tracks and are therefore of comparatively low statistical accuracy.

In the experiment of Kaplon, Noon, and Racette,¹⁰ the measured ratio $R = 18/31 = 0.58$ (at $x = 24 \text{ g/cm}^2$) agrees with other ratios, but the authors have doubled it in order to account for a possible loss of particles when tracing tracks from a sensitive *G-5* to an adjacent less sensitive *C-2* emulsion. They give two arguments for applying this large correction. They measured the number of cases in which an *L* nucleus entered a glass plate in their stack and failed to emerge on the other side. The difference between the observed interaction mean free path of $26 \pm 12 \text{ g/cm}^2$ and the expected value of 42 g/cm^2 was attributed to an occasional failure of the observer to detect the track when it emerges. The indicated statistical error suggests that tracks of *L* nuclei were traced through a total length of 78 g/cm^2 of glass and that three collisions were observed, where only two were expected. The statistical weight of this observation seems insufficient support for the very large correction factor which they have applied to their data. The second argument in favor of the large correction involves equating the probability that a track is missed in a random scan of a *C-2* emulsion (7 tracks were found in an area where 16 were expected) with the probability of missing such tracks in tracing from plate to plate, that is, under conditions when the location, direction, length, and density of the track to be looked for is known in advance. The two probabilities are not directly related and the second is obviously much smaller than the first.

A possible explanation for the comparatively high ratio obtained by Noon, Herz, and O'Brien²⁵ suggests itself if one compares their charge spectrum with that of Waddington,²⁶ Cester *et al.*,²⁸ or our own. The spectra are identical if all the charge values (except that of the lithium peak) could be increased by one unit. The procedure used for charge calibration in that paper is not given in great detail. The main evidence seems to rest on one boron nucleus identified from the number of fragments into which it breaks up. It seems that about 50 δ rays were counted on this track. If one adds to the corresponding statistical uncertainty the uncertainty due to the unknown energy of the particle [see Fig. 9(a), Appendix II], the error becomes larger than the separation in δ -ray density between boron and

carbon. On the hypothesis that such an error in calibration may have occurred, the value of Noon *et al.*, which was obtained in the same balloon flight in which our stack was exposed, is in very good agreement with our and other values.

Fay²⁰ observes in his experiment a strong and unexplained asymmetry in the number of particle tracks. More than twice as many particles enter his stack from the left than from the right. Such an asymmetry would occur if during exposure the package had been tilted with respect to the vertical by an amount corresponding to a rotation through about 30° in the plane of the emulsion. A similar tilt in the direction perpendicular to the face of the emulsions would lead to an average increase of air traversed by the particles of 5–6 g/cm² and this would be sufficient to bring Fay's measurements into agreement with the other data.

APPENDIX V. EXTRAPOLATION OF THE FLUX RATIO L/S TO THE TOP OF THE ATMOSPHERE

The ratio of tracks of L and S nuclei incident under zenith angle θ and registered during a flight of duration T is given by

$$\frac{l(\theta)}{s(\theta)} = \int_0^T L(p, \theta) dt / \int_0^T S(p, \theta) dt, \quad (7a)$$

where $p(t)$ is the atmospheric pressure as a function of time and is given by the flight curve Fig. 7. Except for a common factor which depends on θ but not on p , L and S are functions of $p(t)/\cos\theta = y(t)$ only. We can therefore write

$$\frac{l}{s} = \int_0^T L(y) dt / \int_0^T S(y) dt. \quad (7b)$$

The flight period can be divided in two parts:

(a) The ascent period when the balloon rises at a constant rate $\rho = dh/dt$, and $y(t)$ is given by the differential equation $dy/y = -\rho dt/h_0$. Here h_0 is defined by the relation connecting altitude h with atmospheric pressure p ($p = p_0 e^{-h/h_0}$), and has the value 7.70 km.

(b) A period of duration ΔT during which the balloon floats at a constant pressure P , and where, therefore, $y(t)$ is independent of time t . Thus we can write

$$r(x) = \frac{l(x)}{s(x)} = \left(L(x) + \frac{1}{\beta} \int_x^\infty \frac{L(y)}{y} dy \right) / \left(S(x) + \frac{1}{\beta} \int_x^\infty \frac{S(y)}{y} dy \right) \quad \text{for } x \geq P, \quad (7c)$$

where x is defined by $x = P/\cos\theta$ and β is a parameter which measures the floating period in terms of the

duration of the ascent, $\beta = \rho \Delta T / h_0$. (In our flight, $\rho = 3.32$ m/sec and $\Delta T = 6\frac{1}{4}$ hours; therefore $\beta = 9.73$.)

Since $S(x)$ comprises all nuclei heavier than L nuclei, no additional S nuclei are produced in the atmosphere, and (as shown in Sec. V) the S component is absorbed exponentially. Therefore, $S(x)$ and $L(x)$ satisfy the differential equations

$$dS/dx = -S/\Lambda_S, \quad S = S_0 e^{-x/\Lambda_S}; \quad (8a)$$

$$dL/dx = -(L/\Lambda_L) + kS,$$

$$L = L_0 e^{-x/\Lambda_L} + k\Lambda_S S_0 (e^{-x/\Lambda_L} - e^{-x/\Lambda_S}); \quad (8b)$$

$$1/\Lambda = (1/\Lambda_S) - (1/\Lambda_L).$$

We designate by $R_0 = L_0/S_0$ the flux ratio of L and S nuclei at the top of the atmosphere and use the abbreviations

$$U_S = e^{-x/\Lambda_S} + \frac{1}{\beta} \int_x^\infty \frac{e^{-y/\Lambda_S}}{y} dy, \quad (9a)$$

$$U_L = e^{-x/\Lambda_L} + \frac{1}{\beta} \int_x^\infty \frac{e^{-y/\Lambda_L}}{y} dy, \quad (9b)$$

$$f = (U_L/U_S) - 1. \quad (9c)$$

Upon using these symbols, Eq. (7c) becomes

$$r(x) = R_0(f+1) + k\Lambda f. \quad (7d)$$

One can eliminate the unknown parameter k by using Eq. (7d) as well as its derivative with respect to x . One obtains

$$R_0 = r(x) - r'f/f', \quad (10a)$$

where prime denotes differentiation with respect to x . If we choose x to lie in the interval for which we have good experimental data, $r(x)$ can be approximated by the line of least square deviation from the experimental data. Then $r(x) = r_0 + \alpha x$, where r_0 is the intercept and α the slope of the straight line. Equation (10a) then becomes

$$R_0 = r_0 - \alpha \left(\frac{f}{f'} - x \right) = r_0 - \alpha \delta, \quad (10b)$$

which connects the extrapolated flux value with the intercept and slope of the line fitting the uncorrected data.

Equation (10b) gives the correct extrapolation of flux ratios for all balloon experiments and is applicable whenever the ratio and its derivative is known at some atmospheric depth x .

We calculate f/f' by using the values of absorption mean free paths given in Sec. V, namely $\Lambda_S = 29 \pm 1$ g/cm², $31.5 < \Lambda_L < 33.5$. For x we may choose either the median value $\bar{x} = 11.2$ g/cm² (half of all tracks traverse less than \bar{x}), of the average value $\langle x \rangle = 14.6$ g/cm² (defined by $\langle x \rangle = \sum_{i=1}^N x_i/N$). The correction term δ may be separated into two components,

TABLE IV. Correction terms for the extrapolated ratio.

	$\Lambda_S = 28 \text{ g/cm}^2$ $\Lambda_L = 33.5 \text{ g/cm}^2$		$\Lambda_S = 29 \text{ g/cm}^2$ $\Lambda_L = 32.5 \text{ g/cm}^2$		$\Lambda_S = 30 \text{ g/cm}^2$ $\Lambda_L = 31.5 \text{ g/cm}^2$	
	δ_c	δ_a	δ_c	δ_a	δ_c	δ_a
$x = \bar{x} = 11.2 \text{ g/cm}^2$	-0.40	2.05	-0.25	2.15	-0.10	2.25
$x = \langle x \rangle = 14.6 \text{ g/cm}^2$	-0.60	1.80	-0.40	2.0	-0.15	2.05

$\delta = \delta_c + \delta_a$, where δ_c arises from the fact that the growth curve deviates from a straight line and δ_a arises from the finite rate of ascent. δ_c can be calculated by letting

β in Eqs. (9a) and (9b) go to infinity. One finds $\delta_c = \Lambda[1 - (x/\Lambda) - e^{-x/\Lambda}]$, where $1/\Lambda = (1/\Lambda_S) - (1/\Lambda_L)$. δ_a is then given by $\delta_a = \delta - \delta_c$. In Table IV, we give the correction term for various values of assumed absorption mean free paths and both values, \bar{x} and $\langle x \rangle$. We see that, as expected, δ is not very sensitive to the choice of the exact value x at which the straight line is fitted to the growth curve. However, the median value \bar{x} seems to be the more reasonable choice and we therefore shall use

$$\delta = \delta_c + \delta_a = 1.90 \pm 0.25 \text{ g/cm}^2. \quad (11)$$

Multiple Production of Pions in Nuclear Collisions*

PREM PRAKASH SRIVASTAVA, *Physics Department, Tufts University, Medford, Massachusetts*

AND

GEORGE SUDARSHAN,† *Physics Department, University of Rochester, Rochester, New York*

(Received January 13, 1958)

The statistical theory of meson production in nuclear collisions is given a fully covariant formulation. A single parameter of the dimensions of a mass appears in the theory, which is normalized by matching a single experimental number. Numerical results for various processes are presented. A simple recurrence relation between the covariant phase-space integrals greatly facilitates the computations.

WE have attempted to calculate the relative transition probabilities of multiple meson processes by using a covariant statistical theory. The starting point is a reduction of the transition probability into a form in which the kinematic factors are separated out and the matrix element of an ordered product of field operators occurs as an unknown function. The statistical assumption¹ now permits an evaluation of the relative transition probabilities. The relative probabilities thus obtained are in much better agreement with the experimental findings than the predictions from various versions of the statistical theory already discussed by several authors.² Comprehensive calculations have been made of multiple meson production in nucleon-nucleon collisions, nucleon-pion collisions, and nucleon-antinucleon annihilation. A short summary of some of the results is presented below.

The relative transition probability for a final state involving two nucleons of four-momenta p_1 and p_2 and m pions of four-momenta q_1, q_2, \dots, q_m starting from an initial state of two nucleons of four-momenta p_1' and

p_2' can be written in the form³

$$W_m = \int d^4p_1 d^4p_2 d^4q_1 \dots d^4q_m \delta^4(p_1 + p_2 + q_1 + \dots + q_m - p_1' - p_2') \delta(p_1^2 - m^2) \delta(p_2^2 - m^2) \times \delta(q_1^2 - \mu^2) \dots \delta(q_m^2 - \mu^2) f(p, p', q).$$

Here $f(p, p', q)$ is an invariant function of the nucleon and pion four-momenta, and is obtained by averaging over initial spins and summing over the final spins the absolute square of the matrix element. Since all the external lines considered correspond to real noninteracting particles, we have the relations

$$p'^2 = p^2 = m^2, \quad q^2 = \mu^2.$$

The statistical theory is obtained by replacing $f(p, p', q)$ by a constant quantity independent of the four-momenta but depending on the number of meson (and nucleon) lines in the diagram. Dimensional considerations lead to the form

$$f(p, p', q) = AS(m)\kappa^{-2m},$$

where κ is a quantity of the dimensions of a mass and A is a numerical constant. Since we are interested in the relative transition probability only, the constant A

* Supported in part by the U. S. Atomic Energy Commission.
† On leave of absence from Tata Institute of Fundamental Research, Bombay, India.

¹ E. Fermi, *Progr. Theoret. Phys. (Japan)* **5**, 570 (1950).
² E. Fermi, *Phys. Rev.* **92**, 452 (1953); *Phys. Rev.* **93**, 1434 (1954); R. H. Milburn, *Revs. Modern Phys.* **27**, 1 (1955); J. V. Lepore and M. Neuman, *Phys. Rev.* **98**, 1484 (1955); J. S. Kovacs, *Phys. Rev.* **101**, 397 (1956).

³ Schweber, Bethe, and de Hoffmann, *Mesons and Fields* (Row, Peterson and Company, New York, 1955), Vol. I.